Title

RARE GAS-HALOGEN ATOM INTERACTION POTENTIALS FROM CROSSED MOLECULAR BEAMS EXPERIMENTS: I(2p3/2) + Kr, Xe (1S0)

Authors

Casavecchia, P.
He, G.
Sparks, R.K.
et al.

Publication Date

1982-03-01

LBL-14261
Preprint

Lawrence Berkeley Laboratory
UNIVERSITY OF CALIFORNIA

Materials & Molecular
Research Division

Submitted to the Journal of Chemical Physics

RARE GAS-HALOGEN ATOM INTERACTION POTENTIALS FROM CROSSED MOLECULAR BEAMS EXPERIMENTS: $I(^{2p}3/2)$ + Kr, Xe ($^1S_0$)

Piergiorgio Casavecchia, Guozhong He,
Randal K. Sparks, and Yuan T. Lee

March 1982

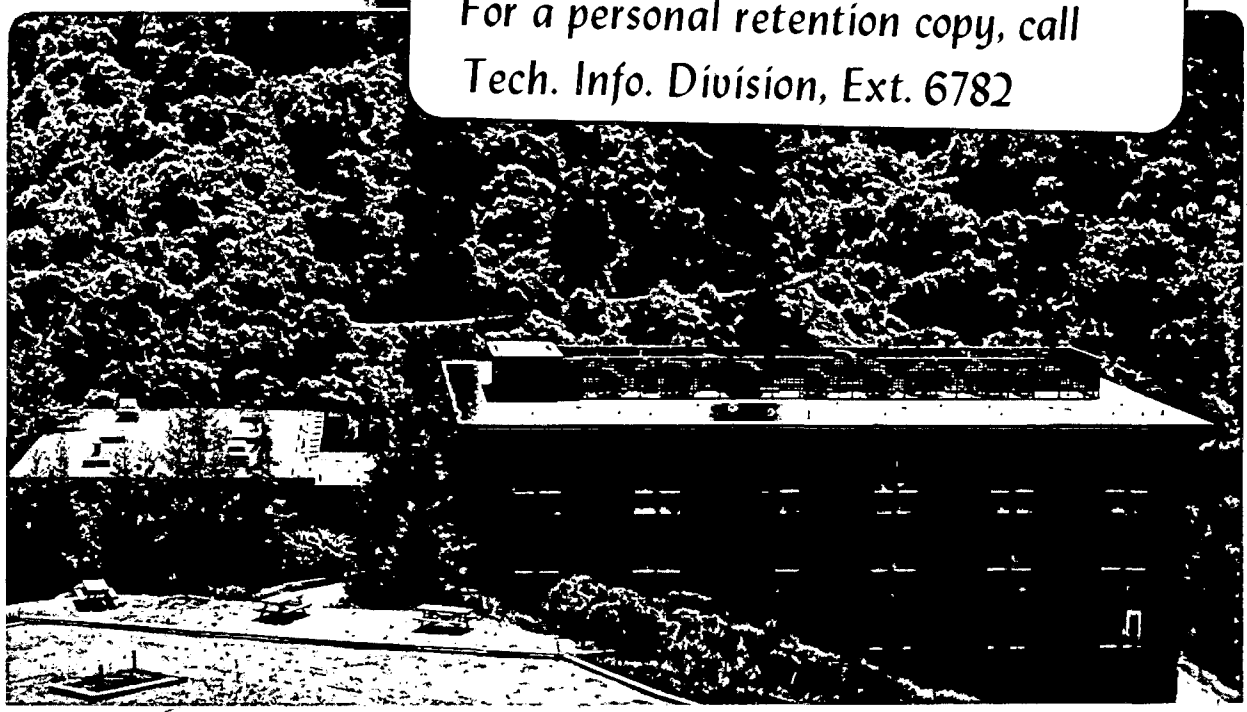

Prepared for the U.S. Department of Energy under Contract DE-AC03-76SF00098

DISCLAIMER

RARE GAS-HALOGEN ATOM INTERACTION POTENTIALS FROM CROSSED MOLECULAR BEAMS EXPERIMENTS: $I(^2P_{3/2})$ + Kr, Xe $(^1S_0)$

Piergiorgio Casavecchia,[a] Guozhong He,[b] Randal K. Sparks[c] and Yuan T. Lee[d]

Materials and Molecular Research Division
Lawrence Berkeley Laboratory and
Department of Chemistry
University of California
Berkeley, California 94720 USA

ABSTRACT

Angular distributions of $I(^2P_{3/2})$ scattered off Kr and Xe $(^1S_0)$ in the thermal energy range have been measured in crossed molecular beams experiments. The interaction potentials for two relevant states (X 1/2 and I 3/2) for each of the systems are obtained by using an approximate elastic scattering analysis, which neglects nonadiabatic coupling, as previously done for other rare gas-halogen systems. The I-Xe (X 1/2) potential (ϵ = 0.69 kcal/mole, r_m = 4.30 Å) and to some extent, I-Kr (X 1/2) potential (ϵ = 0.55 kcal/mole, r_m = 4.05 Å) shows a slightly more attractive interaction than the interaction potentials of Xe-Xe and Xe-Kr, but the I-Xe (I 3/2) potential (ϵ = 0.48 kcal/mole, r_m = 4.60 Å) and the I-Kr (I 3/2) potential (ϵ = 0.36 kcal/mole, r_m = 4.32 Å) present shallower ϵ's, a larger r_m and stronger repulsive walls than the corresponding rare gas pair potentials. The results obtained from this and previous investigations are reviewed.

---

a. Permanent address: Dipartimento di Chimica dell'Universita, 06100 Perugia, Italy.
b. Permanent address: Institute of Chemical Physics, Darien, People's Republic of China.
c. Permanent address: Division of Chemistry and Chemical Engineering, California Institute of Technology, Pasadena, California 91125.
d. Miller Professor, 1981-1982.

INTRODUCTION

Since the first synthesis of rare gas compounds in 1962,[1] much work has been devoted to extend the scope of rare gas chemistry. While in the sixties the major effort was in the preparation and the characterization of polyatomic compounds, in the seventies, following the observation of U.V. emission from rare gas monohalides (RG-X)[2] and the achievement of laser action in XeBr, KrF, XeCl, XeF, ArF and KrCl,[3] a great deal of attention has been paid to diatomic systems.

Although the interaction potentials of excimer states of the RG-X systems, which are similar to ground state alkali halides, have been fairly well characterized in both theoretical[4-7] and experimental investigations,[2,8-10] the determination of the interaction potentials of the ground state has not been as extensive. Knowledge of the interaction of a halogen atom with a rare gas atom in the ground state is important from many reasons. In addition to their usefulness for the understanding of both the emission spectra and the kinetics of lasing action, they are important in understanding the transition from a van der Waals force to a chemical bond. Also, this information is essential to the theoretical study of termolecular recombination of halogen atoms in a rare gas environment.[11] Moreover, the collisions of atoms carrying orbital and spin angular momenta are of interest in the field of scattering theory.

In our earlier crossed molecular beam studies, the attractive potential wells for the X 1/2 state of F-Xe[12] and Cl-Xe[13] derived from differential cross section measurements were found to be in good agreement

with those determined spectroscopically.[14-16] These are the only two systems where bound-to-bound transitions have been observed. In a subsequent series of studies, systems including F-Kr, Ar, Ne[17] and Br-Xe, Kr, Ar[18] were investigated. In this paper, we report our crossed molecular beam investigation on the interaction potentials of I-Xe, Kr systems from the measurements of differential cross sections.

Information on the interactions between iodine and rare gas atoms is quite limited. The theoretical understanding of iodine atom recombination in rare gases has suffered in the past from the lack of reliable information on the I-RG interaction potentials.[19] The emission spectra of I-Xe has been studied recently by several groups.[2b,8,10,20,21] Bands assigned to transitions which terminate on the X 1/2, I 3/2 and II 1/2 states were observed in these studies. The first quantitative analysis of the high pressure B → X (III 1/2 → X 1/2) bands in I-Xe by Tellinghuisen et al.,[20] provided information on the slope of the repulsive interaction potential of the X 1/2 state in the Franck-Condon region relative to the predetermined attractive upper state potential. In a recent investigation of the I-Xe bound-free emission spectra,[22] the slightly adjusted theoretical interaction potentials calculated by Hay and Dunning[5b] were used to simulate B → X (III 1/2 - X 1/2), B → A (III 1/2 - II 1/2) and C → A (II 3/2 - I 3/2) transitions in order to gain information about the shapes of the lower state potential. Estimates of the depth and location of the well for the X 1/2, I 3/2 and II 1/2 potentials have been made. Fluorescence[21] has also been observed from KrI, but just like the XeI, no lasing action has been observed. Photodissociative absorption, which

seriously limits the efficiency of XeBr and XeCl lasers[23] is also thought to be the main reason for the failure of observing the laser oscillation. So far, there is no report published on the spectroscopic analysis for the I-Kr system.

The results obtained from the present study extend the quantitative picture of the interaction potentials of the ground state manifold to a large number of diatomic RG-X systems. Systematic comparison of the results obtained for all RG-X pairs will be made. In particular, from the analysis of the rows and columns of the RG-X matrix, the effect of various halogen atoms and rare gas atoms in the subtle transition from van der Waals forces to chemical forces will be examined.

EXPERIMENTAL

The crossed molecular beams apparatus used in this study is a newly designed higher resolution version[24] of the universal molecular beam machine described by Lee et al.[25] Supersonic beams of iodine atoms seeded in a rare gas carrier are crossed with beams of krypton or xenon under single collision conditions at 90° intersection angle in a liquid nitrogen cooled collision chamber maintained at 8×10^{-8} torr. Scattered iodine atoms are detected as a function of the in plane scattering angle, Θ, by a triply differentially pumped rotatable ultra high vacuum quadrupole mass spectrometer detector.

The iodine atoms were produced by thermal dissociation of I_2 in a resistively heated graphite oven described elsewhere.[26] The collision energy, E, was varied by changing the carrier gas for I_2 while keeping the nozzle temperature of the iodine atom beam source at ~1680 K. The two different seeded mixtures which were used were prepared by passing pure krypton or helium diluent gas through a temperature controlled reservoir containing solid iodine. The reservoir temperature was kept at 340 K, which corresponds to an iodine vapor pressure of 7 torr. In order to prevent subsequent condensation of the iodine vapor the gas inlet line to the nozzle was uniformly heated to a temperature of about 390 K.

The velocity distributions of the beams were characterized by time-of-flight (TOF) measurement. Table I gives the seed mixture, stagnation pressure, peak velocity and full-width-half-maximum (FWHM) velocity spread as well as the average collision energies for each set of beam conditions used.

The bond dissociation energy of the iodine molecule is sufficiently low that nearly total dissociation of iodine can be easily achieved. The nozzle temperature has been estimated from the measurement of the velocity distribution of the beam. Under the normal operating temperature (~1680 K), essentially all the iodine atoms are produced in their ground state, $^2P_{3/2}$.

The inelastic scattering forming electronically excited iodine atoms is expected to give negligible contribution to the measured laboratory angular distribution in the energy range investigated, since the $I(^2P)$ spin-orbit (S-O) splitting is as large as 21.7 kcal/mole.[27] Therefore, no attempt was made to detect the fine structure transition ($^2P_{3/2} \rightarrow {}^2P_{1/2}$) by analyzing the velocity of scattered I atoms.

Laboratory angular distributions, $I(\Theta)$, of scattered I atoms were obtained by taking from 4 to 6 scans of 20 sec counts at each angle for the I_2/He seeded mixture and of 40 sec counts for the I_2/Kr seeded mixture. The $I(\Theta)$ were time normalized by periodically returning the detector to an arbitrary reference angle (usually 10°) in order to account for possible long term drifts in beam intensities and detector sensitivity. The rare gas target beam was modulated at 150 Hz by a tuning fork chopper for background subtraction. The other features of experimental detail have been described previously.[18]

RESULTS AND ANALYSIS

Laboratory angular distributions of $I(^2P_{3/2})$ scattered off Xe $(^1S_0)$ and Kr $(^1S_0)$ at two collision energies are presented on a semi-log scale in Figs. 1 and 2, respectively. Exemplary error bars representing two standard deviations of the mean are shown when visible outside the solid circle. The I-Xe data appear somewhat noisier than the I-Kr data especially at the lowest E, because there is interference from the transmission of a small amount of elastically scattered ^{129}Xe at m/e = 127. Although the mass spectrometer was operated at a fairly high resolution it was not possible to completely eliminate the contribution of ^{129}Xe, without substantially reducing the signal coming from elastically scattered ^{127}I. The data have been corrected for the measured contribution of ^{129}Xe.

The $I(\Theta)$ for both systems at the lowest E clearly show the dark side of the rainbow oscillation. At higher E the angular distributions reflect the scattering mainly from the repulsive part of the potentials. The detection of the heavier atom scattered off the light collision partner is responsible for the somewhat unusual shape of the $I(\Theta)$ at large angles in the I-Kr system (Fig. 2). When one detects the heavy particle scattered off a lighter target, particles scattered at two different center-of-mass (CM) angles are observed at the same laboratory angle. As the detector approaches the edge of the elastic Newton circle, the differential cross section shows a rather broad peak in the vicinity of the cutoff angles, within which the heavy particle is kinematically constrained to scatter. This is due to the nature of the transformation Jacobian which relates the

laboratory and CM reference frames.[28] The $I(\Theta)$ shown in Fig. 2 have been truncated near the onset of this peak. This effect has been properly accounted for in the data analysis.

In contrast to lighter halogen atoms, which contain atoms in both $^2P_{3/2}$ and $^2P_{1/2}$ when produced by thermal dissociation, the I + RG experiments, which are entirely due to the $^2P_{3/2}$ state of iodine, are certainly less complicated. The molecular electronic states arising from the four-fold degenerate ground state $I(^2P_{3/2}) + RG(^1S_0)$ asymptote are the doubly degenerate X 1/2 (or I 1/2) and I 3/2 states, in Hund's case c notation. (In Hund's case b and a notation these are designated $^2\Sigma^+_{1/2}$ and $^2\Pi_{3/2}$, respectively.) In this notation the 1/2 or 3/2 represents the Ω quantum number (the projection of the total electronic angular momentum upon the internuclear axis). The procedure of analysis to obtain the X 1/2 and I 3/2 potentials uses an elastic approximation, which has already been successfully applied to the F, Cl and $Br(^2P) + RG(^1S)$ systems.[12,13,17,18] This method will only be briefly discussed here. Since inelastic events are expected to be negligible for the I-RG systems, the total center-of-mass differential cross section can be written as:

$$\sigma_T(\theta) = \sigma_{X\ 1/2}(\theta)/2 + \sigma_{I\ 3/2}(\theta)/2 \qquad (1)$$

where $\sigma_{X\ 1/2}(\theta)$ and $\sigma_{I\ 3/2}(\theta)$ are the elastic differential cross sections for X 1/2 and I 3/2 states. The calculated center-of-mass elastic differential cross sections are transformed to the laboratory

frame, and averaged over the beam velocity and angular resolution distributions to give the calculated $I(\Theta)$. Comparison of calculated $I(\Theta)$ with experimental $I(\Theta)$ provides the basis for evaluation of the interaction potentials.

The validity of the elastic approximation used here is supported by its ability to corroborate accurate spectroscopically determined X 1/2 potentials for F-Xe[14] and Cl-Xe,[16] in the analysis of laboratory differential cross sections and by more rigorous coupled-channel scattering calculations.[27] This model describing the collisions separately on each of the adiabatic potentials, is expected to hold even better for I-RG systems which are characterized by larger S-O splitting. Hund's case c affords a good description of the collision, with Ω being the good quantum number.[29,30]

In the analysis of the experimental results of Figs. 1 and 2, a flexible analytic form (Morse-Morse-switching function-van der Waals) is used for the description of interaction potentials, $V_{X\ 1/2}(r)$ and $V_{I\ 3/2}(r)$. The reduced form of this potential function can be written as:

$$
\begin{aligned}
f(x) &= V(r)/\epsilon \qquad x = r/r_m \\
f(x) &= \exp(2\beta_1(1-x)) - 2\exp(\beta_1(1-x)) && 0 < x \leq 1 \\
&= \exp(2\beta_2(1-x)) - 2\exp(\beta_2(1-x)) = M_2(x) && 1 < x \leq x_1 \\
&= SW(x)\, M_2(x) + (1-SW(x))\, W(x) && x_1 < x < x_2 \\
&= -C_{6r}x^{-6} - C_{8r}x^{-8} = W(x) && x_2 \leq x < \infty
\end{aligned}
$$

and

$$SW(x) = 1/2[\cos[\ (x-x_1)/(x_2-x_1)] + 1]$$

where $C_{6r} = C_6/r_m^6$, $C_{8r} = C_8/r_m^8$, and ϵ and r_m are the depth and position of the potential minimum. The C_6 constants are estimated from the Slater-Kirkwood formula for effective number of electrons[31] and polarizabilities.[32,33] The small anisotropy of the polarizability of the halogen has been neglected; the C_6 constants for the X 1/2 and I 3/2 states are assumed to be the same. This approximation should have a negligible effect in deriving the information on the attractive well, since the differential cross section is not very sensitive to the long range part of the potential. The C_8 constants are estimated from those of Xe-RG (RG=Xe,Kr) systems.[33] The smaller permanent quadrupole-induced dipole R^{-8} induction term is neglected, as are other coefficients of the asymptotic expansion.

The X 1/2 and I 3/2 potentials are determined by fitting the calculated $I(\Theta)$ to the experimental values through the trial and error adjustment of the rest of the potential parameters. Initially, the I 3/2 potential for the two systems was assumed to be very near the corresponding rare gas pair Xe-RG (RG=Xe,Kr). The best fit $I(\Theta)$ are reported as solid lines in Figs. 1 and 2 for I-Xe and I-Kr, respectively. The derived $V_{X\ 1/2,\ I\ 3/2}$ are shown in Figs. 3 and 4, and the potential parameters are listed in Table II, where those of the Xe-Xe[34] and Xe-Kr[35] systems are also included for comparison. The contribution to $I(\Theta)$ by each of the two potentials is also shown at lowest E in Figs. 1 and 2. The relative weights from Eq. (1) are used in the $I(\Theta)$ plots.

Uncertainties in the ϵ and r_m parameters are obtained by systematically varying the parameters and observing when the $I(\Theta)$ fits become poor. The estimated maximum uncertainties are within ±10% in ϵ and r_m for both $V_{X\ 1/2}$, $V_{I\ 3/2}$ of I-Xe and I-Kr. Possible errors in the Morse β parameters are likely to be of a similar magnitude, based on their observed influence on the $I(\Theta)$ during the fitting procedure. Sensitivity to the repulsive walls is less than that for the well region owing to worse signal-to-noise for the structureless wide angle $I(\Theta)$. Of course, there is no information gained from the experiment about the repulsive walls above the highest collision energy studied. Also, in order to uniquely determine the two interaction potentials involved in the scattering, it is absolutely necessary to use measurements of $I(\Theta)$ at more than one collision energy and covering a wide angular range.

DISCUSSION

In an early study of the XeI emission bands by Ewing and Brau,[8,10] the observed wavelength and spectral width were used to estimate the ground state interaction potential at a distance equal to the potential minimum of the upper state, R_e'. Noting the similarity of the emitting excited XeI and CsI, the potential energy gradient of 1.9 (kcal/mole)$Å^{-1}$ was obtained at 3.3 Å for X 1/2 state.

Tellinghuisen et al.[20] analyzed strong diffuse emission band B → X of XeI quantitatively through a trial and error theoretical simulation, and derived a steeper potential energy gradient in the Franck-Condon region. Their values are

$$-dV_{X\ 1/2}\ (R = 3.31\ Å)/dR = 7.2 \pm 0.6\ \text{(kcal/mole)}\ Å^{-1}$$

$$V_{X\ 1/2}(R = 3.31\ Å) = 1.8 \pm 0.6\ \text{kcal/mole.}$$

The truncated Rittner potential was used for the upper state with ω_e' very close to that of Ref. 8.

Tamagake et al.[22] have also carried out a detailed analysis of the XeI emission spectrum. In their spectral simulation, the ab initio upper ionic state potential[5b] fitted to a Rittner type potential was used, but the ab initio potentials of the ground state manifold were found to be too steep with respect to the upper state potential and required the addition of a dispersion term (R^{-6}) to reach a good agreement. The following values were obtained:

$$-dV_{X\ 1/2}\ (R = 3.585\ \text{Å})/dR\ =\ 6.5\ (\text{kcal/mole})\text{Å}^{-1}$$

$$V_{X\ 1/2}(R = 3.585\ \text{Å})\ =\ 1.14\ \text{kcal/mole.}$$

These values, reflecting the relation between the upper state and X 1/2 state potentials, agree reasonably well with the results of Tellinghuisen et al.,[20] but a with different R_e' value used in the analysis. ε's and r_m's for three potentials in the ground state manifold were also estimated. They are 0.458, 0.157, 0.234 kcal/mole and 4.34, 5.12, 4.80 Å for the X 1/2, I 3/2 and II 1/2 state respectively.

The repulsive wall of XeI $V_{X\ 1/2}$ (r) obtained from the present study gives:

$$-dV_{X\ 1/2}\ (R = 3.31\ \text{Å})/dR\ =\ 7.1\ \text{kcal/mole}\ \text{Å}^{-1}$$

and

$$V_{X\ 1/2}(R = 3.31\ \text{Å})\ =\ 1.43\ \text{kcal/mole.}$$

At a distance equal to R_e' = 3.585 Å, these values become:

$$-dV_{X\ 1/2}\ (R = 3.585\ \text{Å})/dR\ =\ 3.3\ \text{kcal/mole}\ \text{Å}^{-1}$$

and

$V_{X\ 1/2}$ (R = 3.585 Å) ≃ 0.1 kcal/mole.

Our values appear to be in good accord with the spectroscopic estimate of Tellinghuisen et al.,[20] but not with the results of Tamagake et al.[22] The larger ε values (by about 0.3 kcal/mole) of the present study than those of Tamagake et al. for both X 1/2 and I 3/2 states also suggests that their upper B(III 1/2) curve should be moved to shorter internuclear distances. This is actually not surprising, since it has been already observed from a comparison of calculated ω_e', D_e' and R_e' with experimentally derived values for many other rare gas halide systems, that while a fairly good agreement is found between values of ω_e', the calculated values of R_e' are systematically larger by 0.2 - 0.4 Å and the values of D_e' systematically lower.[6] The R_e' value of 3.31 used for the III 1/2 state of I-Xe in the spectrum simulation of Tellinghuisen et al. is 0.01 Å shorter than the R_e' for CsI and is significantly shorter than the theoretical value[5b] of 3.62 Å, which was used by Tamagake et al. Similar disagreement was seen for the Br-Xe system, between our previous molecular beam studies[18] and the analysis of Tamagake et al.

Our results for the I-Xe system show that the $V_{X\ 1/2}(r)$ has a stronger attractive interaction than that of Xe-Xe.[34] The well depth is about 0.13-0.14 kcal/mole (~25%) deeper and r_m about 0.1 Å shorter. Also, the I-Xe inner wall appears to be much less repulsive. A similar trend is observed for the $V_{X\ 1/2}(r)$ of I-Kr compared to Xe-Kr,[35] but the deviations appear to be more modest, being only 0.085 kcal/mole deeper

(~18%) and 0.07 Å shorter. In contrast to $V_{X\ 1/2}$, the $V_{I\ 3/2}$ for both systems deviate in the opposite direction with respect to the corresponding rare gas pair. The ϵ values are shallower by about 0.08 and 0.10 kcal/mole for I-Xe and I-Kr, respectively, the r_m are larger by ~0.2 Å, and the inner wall is slightly more repulsive than for the interaction potentials of Xe-Xe and Xe-Kr.

Recombination data have also been used to estimate the interaction potentials between iodine atoms and rare gas atoms. But, the derivation of reliable detailed information from the highly averaged kinetic rate constants is difficult, especially, when the theory of termolecular recombination used for the analysis is not exact. Porter and Smith[19b] used a simple model and obtained a well depth of 1.3 kcal/mole for I-Xe, which is more than twice as deep as the value obtained in this work. Wong and Burns[19d] studied the iodine atom recombination in a wide range of temperatures using classical trajectory calculations and the Monte Carlo sampling method. Quasibound recombining atom-inert gas complexes were included in their approach. Assuming a Lennard-Jones potential and taking well depths of 0.7, 0.6 and 0.5 kcal/mole for the I-Xe, I-Ar and I-He interaction, respectively, the calculations yielded recombination rate constants in fair agreement with the experiment. By extending the classical trajectory investigation using an improved sampling technique and slightly modified potentials, the agreement between computed and experimental rate constants became reasonable, although not perfect.[19e] The L-J parameters used for these improved calculations are ϵ = 0.7, 0.6, 0.2 kcal/mole and σ = 3.90, 3.55, 3.08 Å for I=Xe, I-Ar and I-He,

respectively. However, in the case of I in He, calculated rate constants failed to reproduce the experimental temperature dependence of the rate constants, and for I in Xe and Ar, the calculated recombination rate constants at low temperatures were significantly lower than experimental results. It is worth noting that in all the theoretical recombination studies, the halogen-rare gas interaction has always been described in terms of a single potential energy curve, of the L-J type. However, the effect of multiple potential curves in systems containing open shell atoms needs careful consideration.[36]

This new and more complete picture of $V_{X\ 1/2}(r)$ and $V_{I\ 3/2}(r)$ for I-Xe and I-Kr may serve the useful purpose of furnishing a reference for refining the excited state potentials in the theoretical simulation of emission spectra as well as for the reevaluation of the theoretical models of termolecular recombination.

The present work on Xe-I and Kr-I not only extends the rare gas halide system to the heaviest combination, it also completes the interesting Xe-X series. ε's and r_m's of the X 1/2 state of all rare gas halide systems studied by the crossed molecular beams method are summarized in Fig. 5 and Fig. 6. Except for the Xe-X series, the values of ε's and r_m's and the general systematic trend are quite similar to those of analogous rare gas-rare gas combinations. For example, in the Kr-X series when the halogen atom becomes heavier both ε and r_m become larger as shown in Fig. 7. In Xe-X series, the deviation from the general trend expected for van der Waals interactions are seen for Xe-Cl and Xe-F as shown in Fig. 8. In the series from Xe-Br to Xe-Cl to Xe-F, the ε

becomes larger instead of smaller. The appearance of a "chemical" nature of the interaction can be seen more clearly when the interaction potentials are plotted in reduced forms. Using ϵ's and r_m's of I 3/2 potentials as reducing parameters, Xe-X potentials of both I 3/2 and X 1/2 states are shown in Fig. 9. Since the interaction of the I 3/2 state is essentially a van der Waals interaction, if the interaction of X 1/2 state of all Xe-X series are also van der Waals interaction, all Xe-X potentials in the X 1/2 state should also be very close together. This is seen to be true only for XeI and XeBr, substantial deviations can be seen clearly for XeCl and XeF.

Comparison of various rare gas halide systems also shows that Xe appears to be chemically more different from Kr, Ar or Ne than F is from Cl, Br or I. Much more extensive variation of the rare gas ionization potentials (21.56 eV for Ne, 15.76 for Ar, 14.0 eV for Kr and 12.13 eV for Xe)[37] than the variations in the electron affinities of the halogen atoms (3.399 eV for F, 3.615 eV for Cl, 3.364 eV for Br and 3.061 eV for I)[38] and the important role played by charge transfer[4] might be the main reason for the peculiar trend in the interaction potential of rare gas halide systems. The small and highly electronegative halogen atom with the most polarizable and most easily ionizable rare gas atom provides the limiting case of F-Xe, which has the strongest interaction potential and clearly indicates the operation of chemical forces beyond the much weaker van der Waals interaction.

ACKNOWLEDGMENTS

This work was supported by the Director, Office of Energy Research, Office of Basic Energy Sciences, Chemical Sciences Division of the U.S. Department of Energy under Contract Number DE-AC03-76SF00098. P.C. acknowledges a fellowship from the Italian Ministry of Education and travel support from NATO Grant No. 1444.

REFERENCES

1. N. Bartlett, Endeavour, 23, 3 (1964).

2. (a) M. F. Golde and B. A. Trush, Chem. Phys. Lett. 29, 486 (1974); (b) J. . Velazco and D. W. Setser, J. Chem. Phys. 62, 1990 (1975).

3. K. Searles and G. A. Hart, Appl. Phys. Lett. 27, 243 (1975); J. J. Ewing and C. A. Brau, Appl. Phys. Lett. 27, 350 (1975); J. A. Mangano and J. H. Jacob, Appl. Phys. Lett. 27, 495 (1975); G. C. Tisone, A. K. Hays, and J. M. Hoffmann, Opt. Commun. 15, 188 (1975); C. A. Brau and J. J. Ewing, Appl. Phys. Lett. 27, 435 (1975); J. M. Hoffman, A. K. Hays, and G. C. Tisone, Appl. Phys. Lett. 28, 538 (1976); J. R. Murray and H. T. Powell, Appl. Phys. Lett. 29, 252 (1976); J. G. Eden and S. K. Searles, Appl. Phys. Lett. 29, 350 (1976).

4. M. Krauss, J. Chem. Phys. 29, 350 (1976).

5. (a) T. H. Dunning and P. J. Hay, J. Chem. Phys. 69, 134 (1978); (b) P. J. Hay and T. H. Dunning, J. Chem. Phys. 69, 2209 (1978).

6. P. J. Hay, W. R. Wadt and T. H. Dunning, Ann. Rev. Phys. Chem. 30, 311 (1979).

7. J. Tellinghuisen and M. R. McKeever, Chem. Phys. Lett. 72, 94 (1980).

8. J. J. Ewing and C. A. Brau, Phys. Rev. A12, 129 (1975).

9. M. F. Golde, J. Mol. Spectr. 58, 261 (1975).

10. C. A. Brau and J. J. Ewing, J. Chem. Phys. 63, 4640 (1975).

11. P. K. Boyd and G. Burns, J. Phys. Chem. 83, 88 (1979).

12. C. H. Becker, P. Casavecchia and Y. T. Lee, J. Chem. Phys. 69, 2377 (1978).

13. C. H. Becker, J. J. Valentini, P. Casavecchia, S. J. Sibener and Y. T. Lee, Chem. Phys. Lett. 61, 1 (1979).

14. J. Tellinghuisen, P. C. Tellinghuisen, J. A. Coxon, J. E. Valazco and D. W. Setser, J. Chem. Phys. 68, 5187 (1978).

15. A. L. Smith and P. C. Kobrinsky, J. Mol. Spectr. 69, 1 (1978).

16. A. Sur, A. K. Hui and J. Tellinghuisen, J. Mol. Spectr. 74, 465 (1979); J. Tellinghuisen, J. M. Hoffman, G. C. Tisone and A. K. Hays, J. Chem. Phys. 64, 2484 (1976).

17. C. H. Becker, P. Casavecchia and Y. T. Lee, J. Chem. Phys. 70, 2986 (1979).

18. P. Casavecchia, G. He, R. K. Sparks and Y. T. Lee, J. Chem. Phys. 75, 710 (1981).

19. (a) G. Porter and J. A. Smith, Nature 184, 446 (1959); (b) G. Porter and J. A. Smith, Proc. R. Soc. A261, 28 (1961); (c) A. G. Clarke and G. Burns, J. Chem. Phys. 55, 4717 (1971); (d) W. H. Wong and G. Burns, J. Chem. Phys. 58, 4459 (1973); (e) D. T. Chang and G. Burns, Can. J. Chem. 54, 2535 (1976); (f) G. Burns and A. W. Young, J. Chem. Phys. 72, 3630 (1980).

20. J. Tellinghuisen, A. K. Hays, J. M. Hoffman and G. C. Tisone, J. Chem. Phys. 65, 4473 (1976).

21. M. P. Casassa, M. F. Golde and A. Kvaran, Chem. Phys. Lett. 59, 51 (1978).

22. K. Tamagake, D. W. Setser and J. H. Kolts, J. Chem. Phys. 74, 4286 (1981).

23. J. J. Ewing, in Chemical and Biochemical Applications of Lasers, edited by C. B. Moore (Academic, New York, 1977), Vol. II, p.241.

24. R. K. Sparks, Ph.D. Thesis, University of California, Berkeley, California, 1979.

25. Y. T. Lee, J. D. McDonald, P. R. LeBreton and D. R. Herschbach, Rev. Sci. Instr. 40, 1402 (1969).

26. J. J. Valentini, M. J. Coggiola and Y. T. Lee, Rev. Sci. Instr. 48, 58 (1977).

27. C. H. Becker, P. Casavecchia, Y. T. Lee, R. E. Olson and W. A. Lester, Jr., J. Chem. Phys. 70, 5477 (1979).

28. R. B. Bernstein and J. T. Muckerman, Adv. Chem. Phys. 12, 389 (1967); Ch. Schlier, Ann. Rev. Phys. Chem. 20 191 (1969); U. Buck, Adv. Chem. Phys. 30, 313 (1975); H. Pauly, in Atom-Molecule Collision Theory, edited by R. B. Bernstein (Plenum, New York, 1979), Chapter 4.

29. V. Aquilanti and G. Grossi, J. Chem. Phys. 73, 1165 (1980).

30. V. Aquilanti, P. Casavecchia, G. Grossi and A. Lagana, J. Chem. Phys. 73, 1173 (1980).

31. J. C. Slater and J. G. Kirkwood, Phys. Rev. 37, 682 (1931); see also K. S. Pitzer, Adv. Chem. Phys. 2, 59 (1959).

32. R. R. Teachout and R. T. Pack, At. Data 3, 195 (1971).

33. J. S. Cohen and R. T. Pack, J. Chem. Phys. 61, 2372 (1974).

34. (a) J. M. Farrar, T. P. Schafer and Y. T. Lee, AIP Conference Proceedings, No. 11, Transport Phenomena (1973, edited by J. Kestin, p.279; (b) J. A. Barker, R. O. Watts, J. K. Lee, T. P. Schafer and Y. T. Lee, J. Chem. Phys. 61, 3081 (1974).

35. C. H. Becker, R. J. Buss and Y. T. Lee, to be published.

36. D. G. Truhlar, J. Chem. Phys. 56, 3189 (1972); J. T. Muckerman and M. D. Newton, J. Chem. Phys. 56, 3191 (1972).

37. C. E. Moore, Atomic Energy Levels, Natl. Bur. Stand. (U.S.) Circ. 467, Vols. I, II and III (1949, 1952, 1958).

38. H. Hotop and W. C. Lineberger, J. Phys. Chem. Ref. Data 4, 539 (1975).

Table I. Beam Characteristics and Center-of-Mass Collision Energies

Beam	Stagnation Pressure (Torr)	Peak Velocity (10^4 cm/s)	$\Delta v/v$ (FWHM)	Average Collision Energies E (kcal/mole) I-Xe	I-Kr
0.9% I_2 + 99.1% Kr	770	9.55	0.17	7.7	6.4
0.9% I_2 + 99.1% He	800	24.69	0.20	47.4	37.4
Xe	200	3.08	0.10		
Kr	300	3.81	0.10		

Table II. Interaction Potential Parameters for I-Xe, Kr and Xe-Xe, Kr.

System	I-Xe		I-Kr		Xe-Xe		Xe-Kr
Electronic State	X 1/2	I 3/2	X 1/2	I 3/2	1_{Σ}^{+}		1_{Σ}^{+}
ϵ (kcal/mole)	0.690	0.480	0.550	0.360	0.548[a]	0.558[b]	0.465[c]
r_m (Å)	4.30	4.60	4.05	4.32	4.45	4.36	4.12
β_1	4.40	7.10	5.70	6.80	6.62		6.00
β_2	6.50	7.30	6.10	6.30	6.475		6.30
x_1	1.1066	1.0950	1.1136	1.1100	1.1071		1.1189
x_2	1.800	1.635	1.850	1.700	1.635		1.370
C_6 (kcal/mole Å^6)	4955.	4955.	3254.	3254.	4145.		2800.
C_8 (kcal/mole Å^8)	34570.	34570	20940.	20940.	28930.		15000.

[a]Ref. 34a.
[b]Ref. 34b. This Xe-Xe potential should be more accurate than that of Ref. 35a. Only ϵ and r_m are reported since the potential is not of the MMSV form. The repulsive walls are similar.
[c]Ref. 35.

FIGURE CAPTIONS

Fig. 1. Laboratory angular distributions of scattered I for the $I(^2P_{3/2}) + Xe(^1S_0)$ system at two collision energies. Solid circles are data points and the solid curves are calculated from the best fit potentials of Table II, averaging over angular and velocity distributions of experimental conditions. Dashed and dashed-dotted curves represent the relative contribution to $I(\Theta)$ of the X 1/2 and I 3/2 potentials of Table II, according to Eq. (1).

Fig. 2. Laboratory angular distributions of scattered I for the $I(^2P_{3/2}) + Kr(^1S_0)$ system at two collision energies. Symbols are the same as in Fig. 1.

Fig. 3. Interaction potentials for $I(^2P_{3/2}) + Xe(^1S_0)$ obtained from experimental results shown in Fig. 1. Note the scale change at V(r) higher than 0.1 kcal/mole.

Fig. 4. Interaction potentials for $I(^2P_{3/2} + Kr(^1S_0)$ obtained from experimental results shown in Fig. 2.

Fig. 5. Well depth, ε, of the X 1/2 potential for the X-RG versus halogen atom.

Fig. 6. Minimum position, r_m, of the X 1/2 potential for the X-RG versus halogen atom.

Fig. 7. Comparison of Kr-halogen interaction potentials for the X 1/2 state.

Fig. 8. Comparison of Xe-halogen interaction potentials for the X 1/2 state.

Fig. 9. Reduced potentials for Xe-halogen systems. ϵ and r_m of I 3/2 potential of each of system was taken as unity.

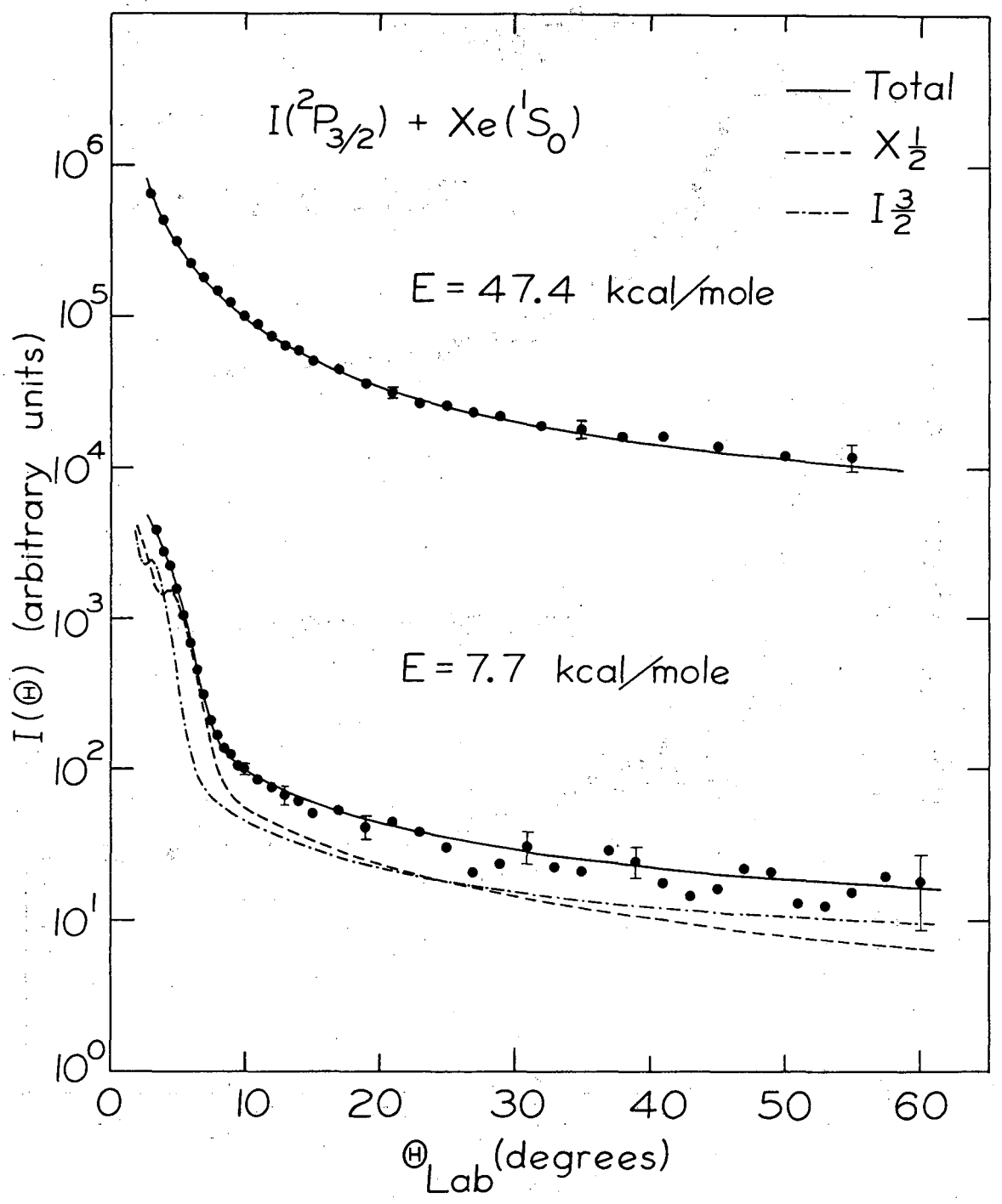

XBL 804-9356

Fig. 1

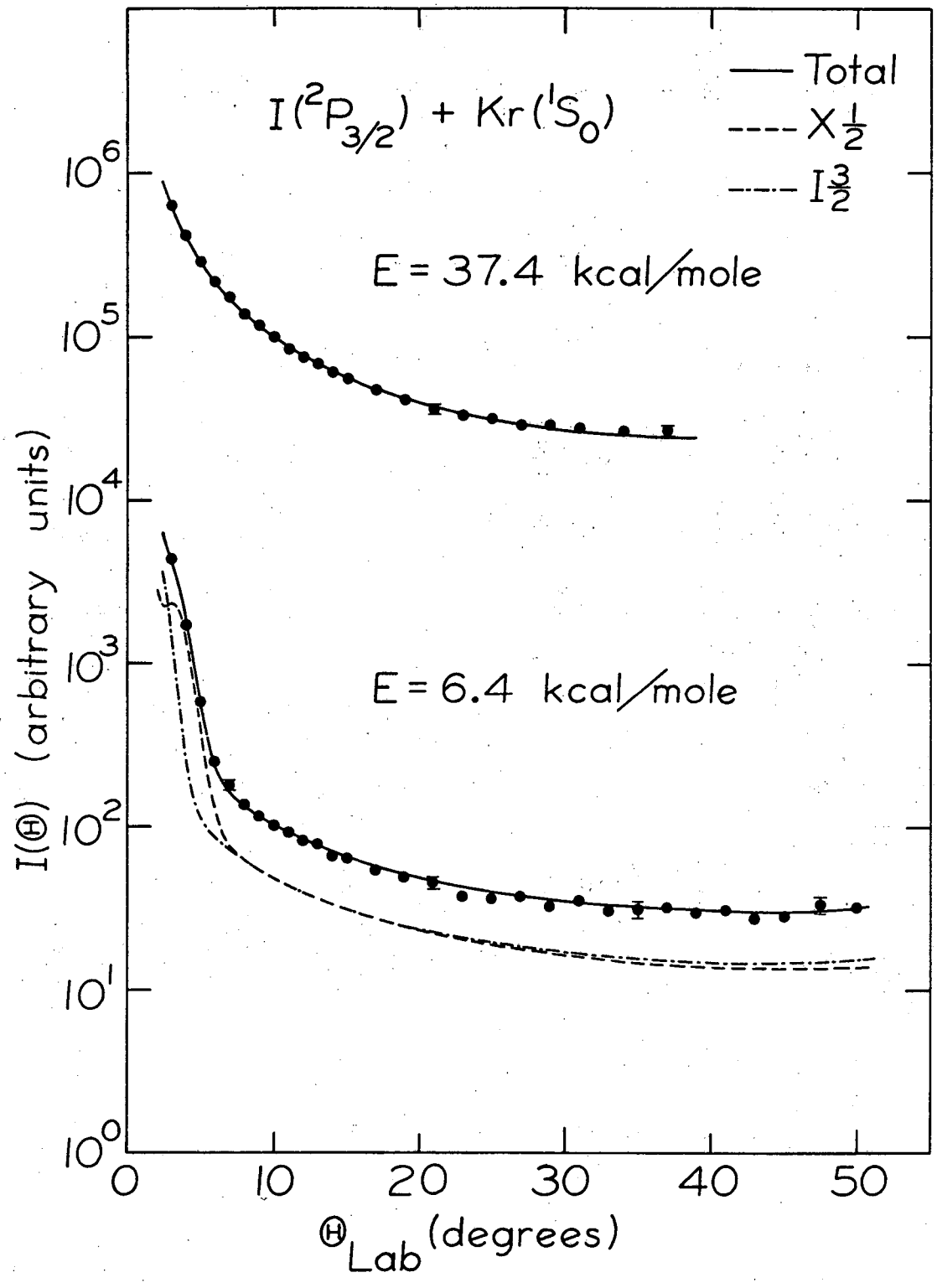

XBL 804-9355

Fig. 2

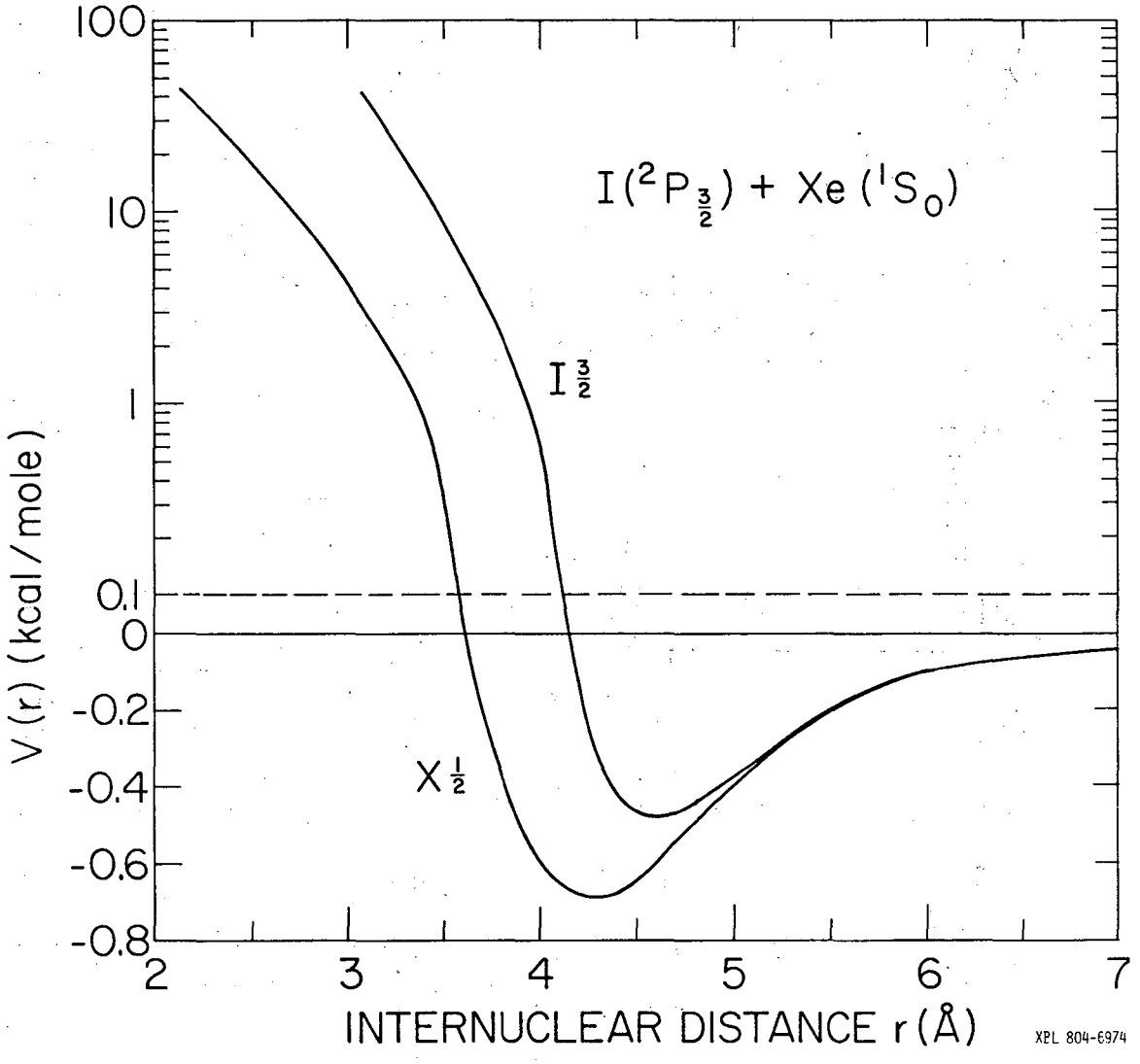
100
10
1
0.1
0
-0.2
-0.4
-0.6
-0.8
V (r) (kcal / mole)
2
3
4
5
6
7
INTERNUCLEAR DISTANCE r (Å)
I(²P 3/2) + Xe (¹S 0)
I 3/2
X 1/2
XPL 804-6974

Fig. 3

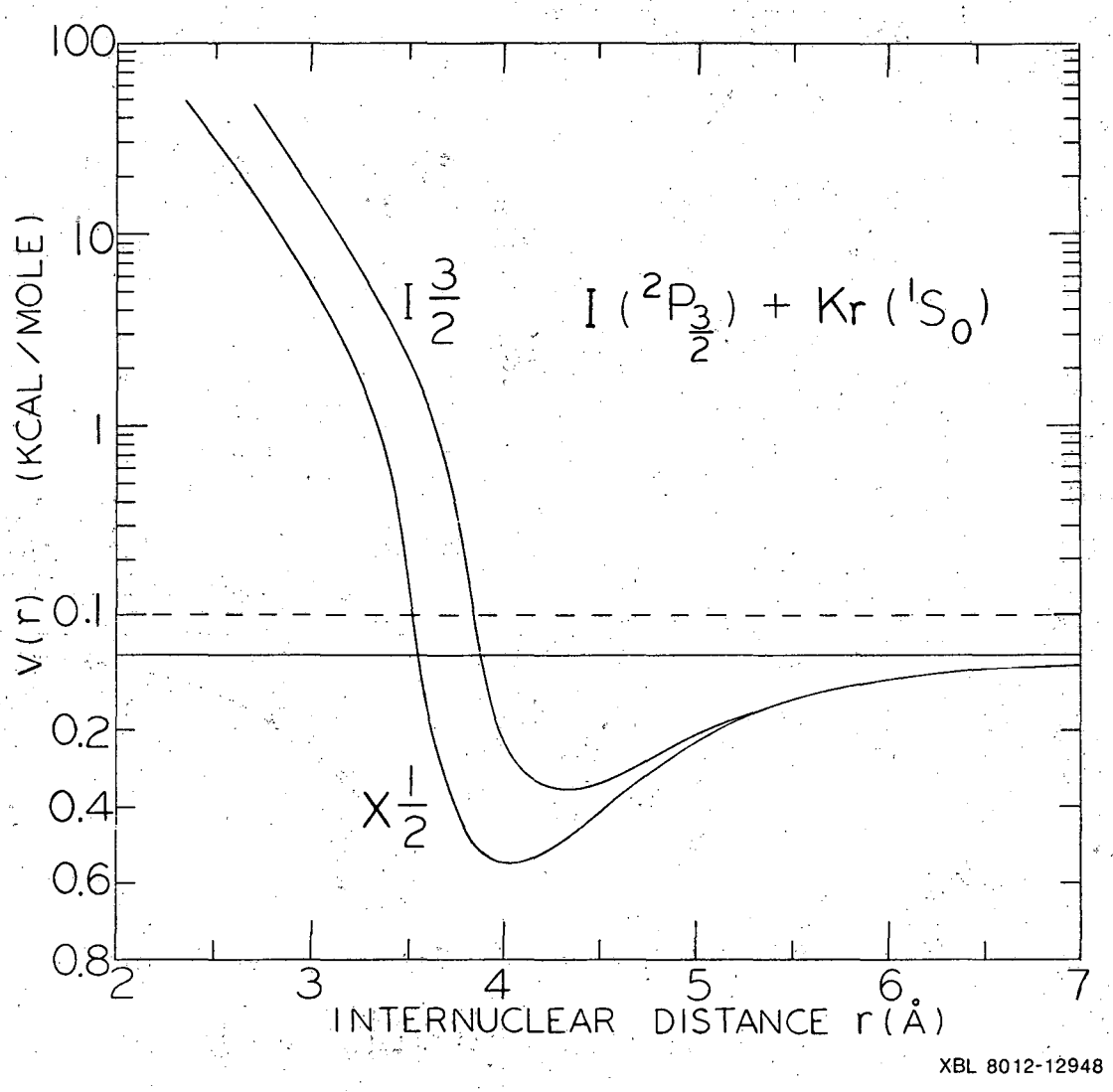
100
10
1
0.1
0.2
0.4
0.6
0.8
V(r) (KCAL/MOLE)
2
3
4
5
6
7
INTERNUCLEAR DISTANCE r(Å)
$I\frac{3}{2}$
$I(^2P_{\frac{3}{2}}) + Kr(^1S_0)$
$X\frac{1}{2}$
XBL 8012-12948

Fig. 4

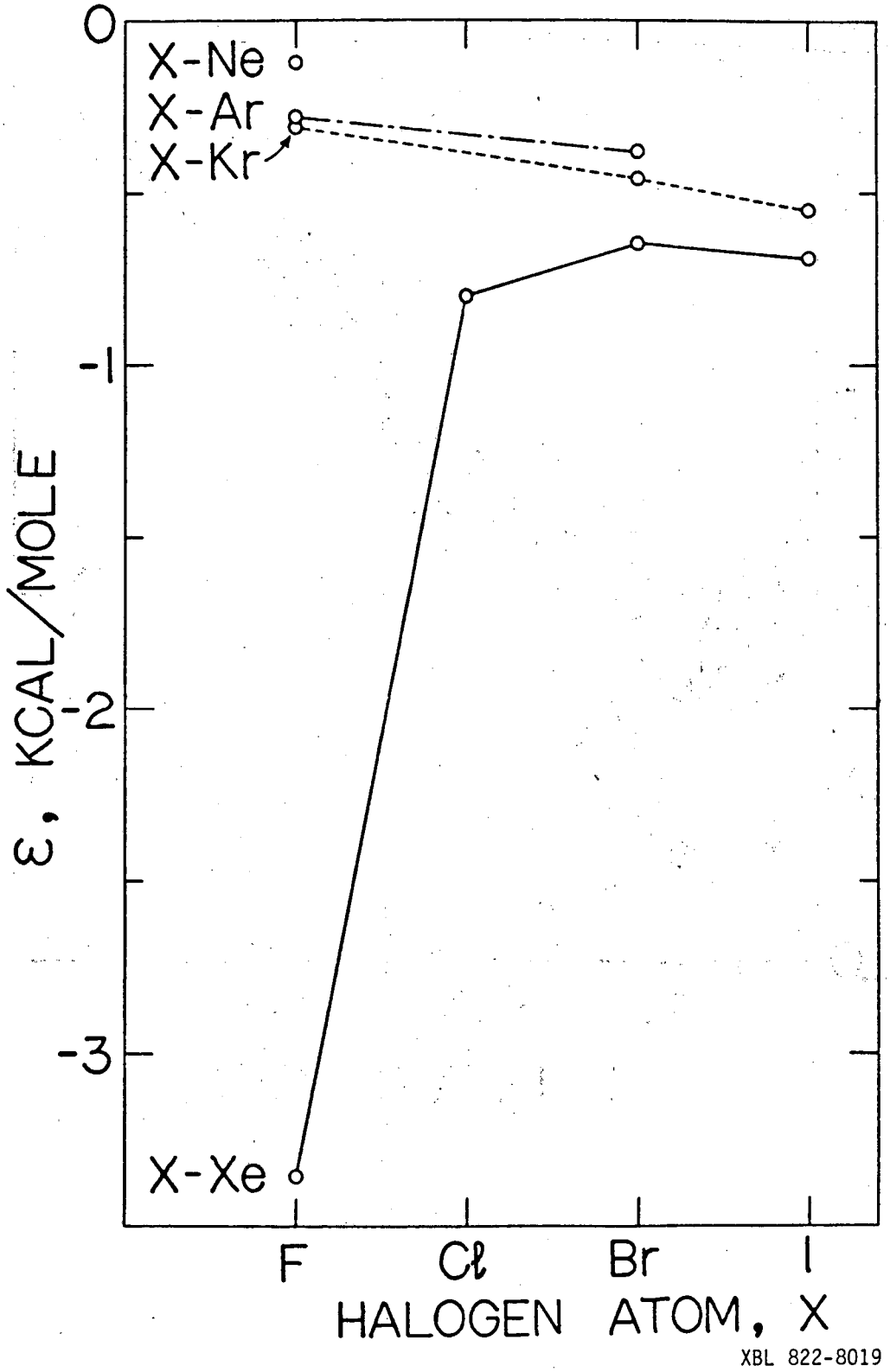
0
-1
-2
-3
X-Ne
X-Ar
X-Kr
X-Xe
ε, KCAL/MOLE
F
Cl
Br
I
HALOGEN ATOM, X
XBL 822-8019

Fig. 5

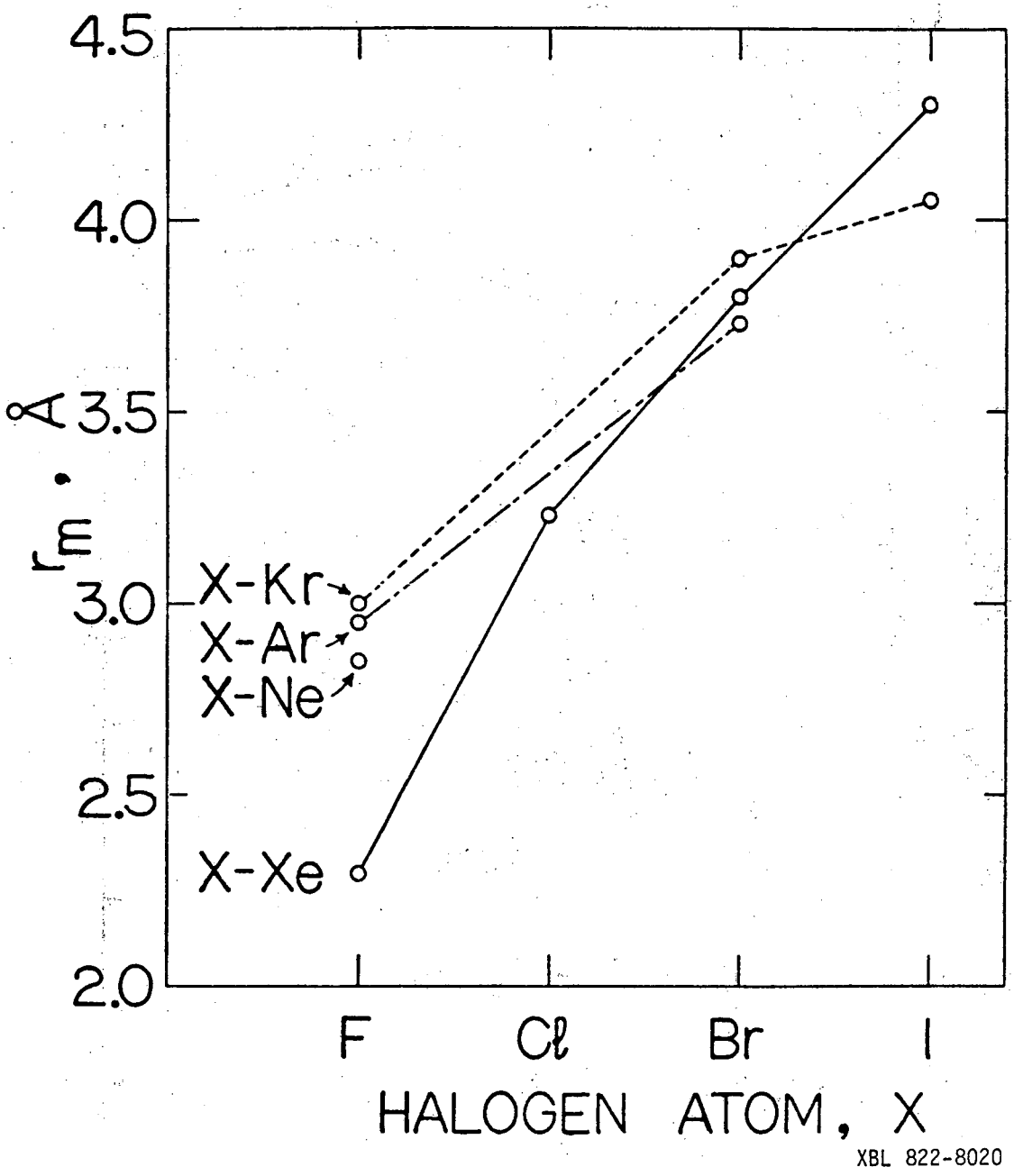
4.5
4.0
3.5
3.0
2.5
2.0
r_E, Å
X-Kr
X-Ar
X-Ne
X-Xe
F
Cl
Br
I
HALOGEN ATOM, X
XBL 822-8020

Fig. 6

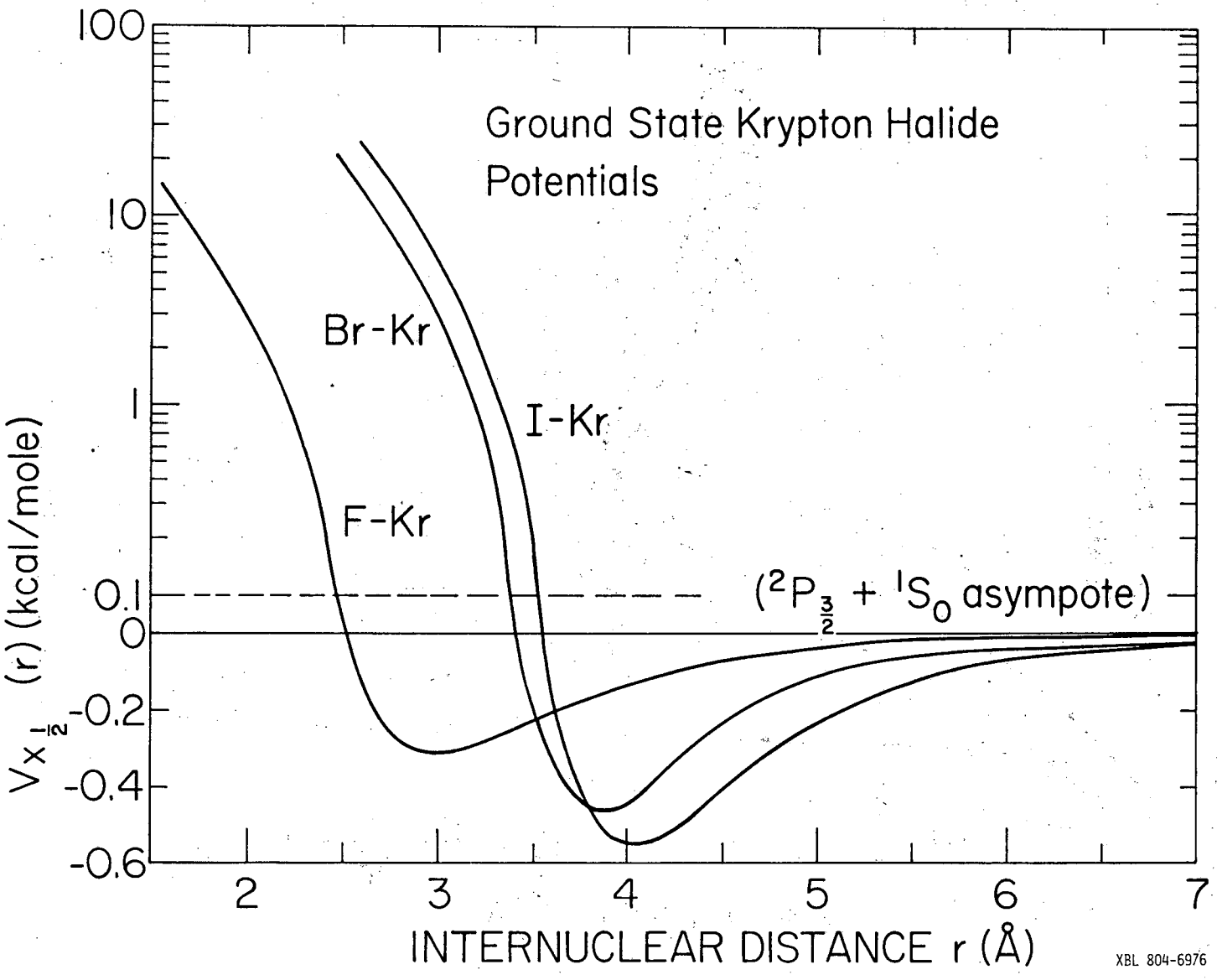
Ground State Krypton Halide Potentials
Br-Kr
I-Kr
F-Kr
$(^2P_{\frac{3}{2}} + {}^1S_0$ asympote)
$V_{X\frac{1}{2}}$ (r) (kcal/mole)
INTERNUCLEAR DISTANCE r (Å)
100
10
1
0.1
0
-0.2
-0.4
-0.6
2
3
4
5
6
7
XBL 804-6976

Fig. 7

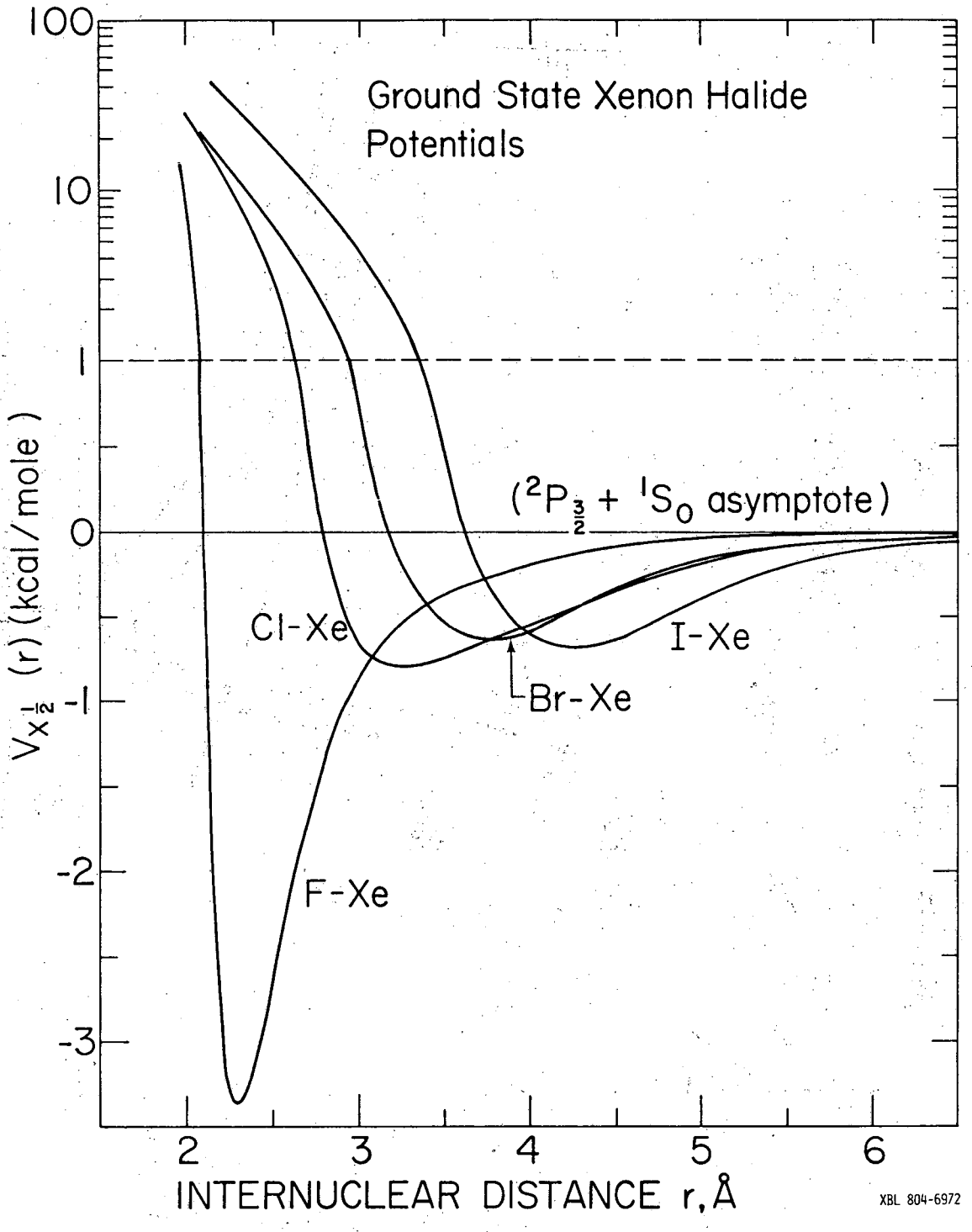
Ground State Xenon Halide Potentials
100
10
1
0
-1
-2
-3
$V_{X\frac{1}{2}}$ (r) (kcal/mole)
($^2P_{\frac{3}{2}}$ + $^1S_0$ asymptote)
Cl-Xe
Br-Xe
I-Xe
F-Xe
2
3
4
5
6
INTERNUCLEAR DISTANCE r, Å
XBL 804-6972

Fig. 8

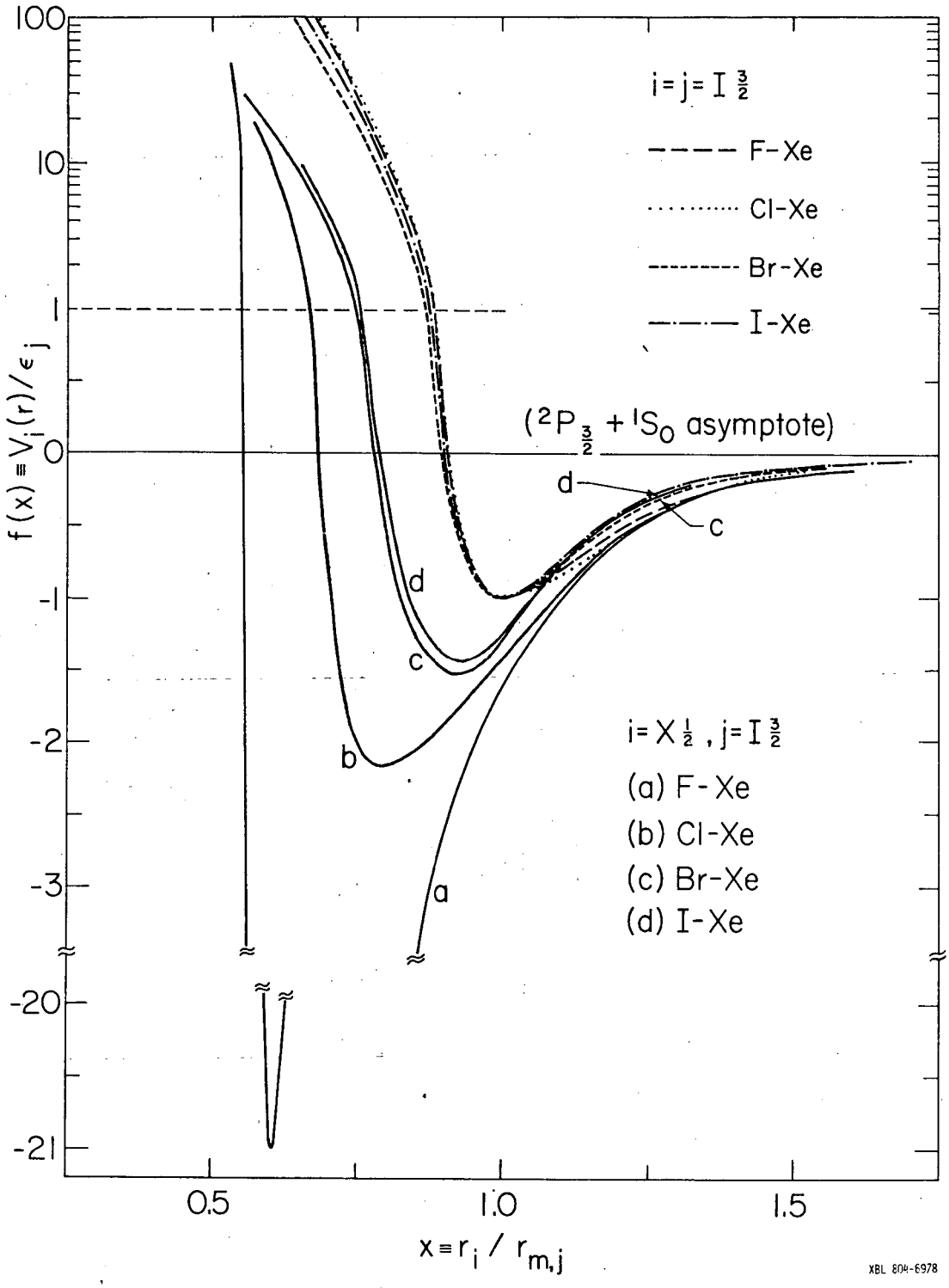
100
10
0
-1
-2
-3
-20
-21
0.5
1.0
1.5
$f(x) \equiv V_i(r)/\epsilon_j$
$x \equiv r_i / r_{m,j}$
$i = j = I\,\frac{3}{2}$
F-Xe
Cl-Xe
Br-Xe
I-Xe
$(^2P_{\frac{3}{2}} + {}^1S_0$ asymptote)
$i = X\,\frac{1}{2}$, $j = I\,\frac{3}{2}$
(a) F-Xe
(b) Cl-Xe
(c) Br-Xe
(d) I-Xe
a
b
c
d
d
c
XBL 804-6978

Fig. 9

This report was done with support from the Department of Energy. Any conclusions or opinions expressed in this report represent solely those of the author(s) and not necessarily those of The Regents of the University of California, the Lawrence Berkeley Laboratory or the Department of Energy.

Reference to a company or product name does not imply approval or recommendation of the product by the University of California or the U.S. Department of Energy to the exclusion of others that may be suitable.

TECHNICAL INFORMATION DEPARTMENT
LAWRENCE BERKELEY LABORATORY
UNIVERSITY OF CALIFORNIA
BERKELEY, CALIFORNIA 94720